Modelling of liquid steel flow with free surface

Marcela B. Goldschmit*, Sergio P. Ferro, A. Heriberto Coppola Owen

Center for Industrial Research, FUDETEC

Av. Simini 250 , 2804 Campana

ARGENTINA

* e-mail: sidgld@siderca.com

Abstract: A finite element turbulence model is developed to simulate the steelmaking processes where the behaviour of an interface between two fluids is relevant. The pseudoconcentration technique is used to distinguish the two fluids and the interface is updated with a smoothing technique. A modified pressure that represents the difference between the actual pressure and the hydrostatic pressure is used. Two steps during the continuous casting process are simulated. One of them is the steel drainage of the ladle in transient state. The other one is the interface between the liquid steel and the liquid casting powder in the slab mold for different submerged entry nozzles.

Keywords: two-fluid interfaces, continuous casting, turbulence modelling, free surface

1. INTRODUCTION

A scheme of the continuous caster is presented in Figure 1. In brief, the process consists of:

- ✓ The ladle pours the liquid steel through the shrouding into the tundish.
- ✓ In the tundish, the liquid steel is distributed through different casting lines.
- ✓ Each casting line is equipped with a refrigerated mold where the steel begins its solidification process.
- ✓ The solidification process continues with water sprays exposition into the secondary cooling chamber.
- ✓ Finally, a torch at the cut-off point cuts the completely solidified steel.

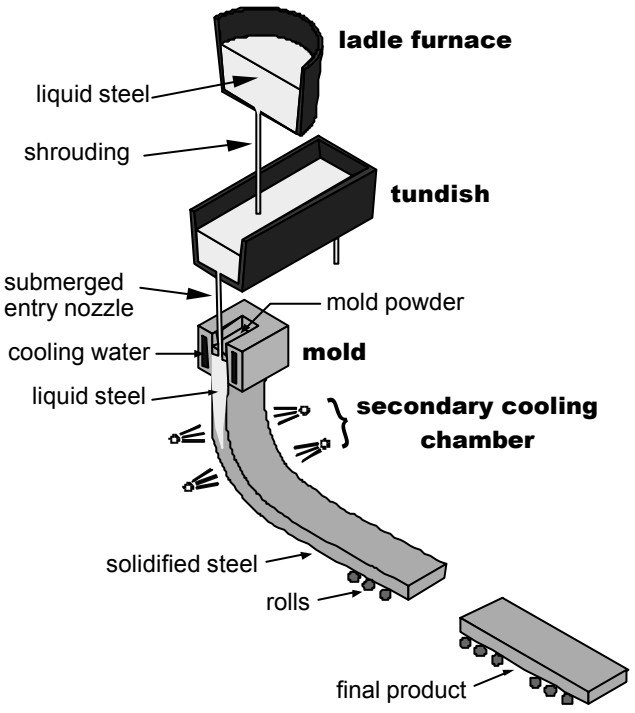

Figure 1 – Scheme of the continuous casting processes

The behaviour of the liquid steel inside the continuous casting process is very complex because it includes: turbulent movement [1], injection of inert gas [2], interfaces between liquid steel and different kinds of slag [3], solidification [4], segregation of chemical components [5], sometimes stirring with electromagnetic forces [6], etc. Then, the liquid steel movement is analysed separately in each of the vessels taking into account only some of the physical mechanisms involved. The flow is mostly analysed using physical or numerical modelling [7] given the difficulty or impossibility of actual measurements in the caster. In general, physical models are scaled versions of the components of the caster where the flow of water is analysed.

In this paper the liquid steel flow and its interfaces with the liquid slag or air (free-surface problems) are numerically analysed with the finite element method. In numerical solutions of flow problems with free surfaces or two-fluid interfaces, the location of the interface is unknown and must be determined as part of the solution. Different methods have been developed in order to solve the problem of tracking the interface. There are basically two different ways to approach the tracking of the interface in computational mechanics:

- ✓ Lagrangian methods [8-9] track the interface by moving the mesh on each time step.
- ✓ Eulerian methods consider an interface function that is advected through a fixed mesh.

Eulerian methods to track interfaces with very similar characteristics may be found in literature with different names: pseudoconcentration method [10-11], interface capturing method [12], marker and cell method [13], level set method [14], colour function method

[15] and so on. The pseudoconcentration method is employed in this paper to describe the behaviour of interfaces in the context of continuous casting of steel.

In Section 2 the numerical model for turbulent flows with interfaces is described. The finite element method with linear interpolation for the velocity and penalisation to impose the incompressibility constraint is used. Two turbulence models are applied: the k-ε model [16] (k is the turbulent kinetic energy, ε is the dissipation rate of turbulent kinetic energy) using our *(k-L)-predictor / (ε)-corrector* algorithm [17-18] and the mixing length model [19].

In Section 3 the numerical model is compared with an experimental water model for the flow inside the mold published in [20-21].

Two industrial applications of the model are commented in Section 4: the behaviour of the interface between liquid steel and molten flux powder in the slab mold with different submerged entry nozzle design, and the liquid steel drainage of the ladle.

Finally, Section 5 is devoted to conclusions.

2. NUMERICAL MODEL FOR TURBULENT FLOWS WITH INTERFACES

Since the liquid steel inside the caster behaves like a Newtonian incompressible fluid, the velocity is a divergence-free field. Therefore, the Navier-Stokes equation may be applied.

However, as the flow inside the continuous caster circulates at a high Reynolds number, the mathematical model requires the addition of turbulence models.

Reynolds-stress models are commonly used to model turbulent flow in industrial applications. In these models the unknowns are decomposed in two terms: one representing mean values and the other one representing the turbulent fluctuations [19]. Navier Stokes equations are solved in terms of the mean values, as follows:

$$\tilde{\mathbf{N}} \cdot \mathbf{v} = 0 \tag{1}$$

$$r \frac{\partial \mathbf{v}}{\partial t} + r\mathbf{v} . \tilde{\mathbf{N}}\mathbf{v} - \tilde{\mathbf{N}} \cdot \left[\left(m + m^t\right)\left(\tilde{\mathbf{N}}\mathbf{v} + \tilde{\mathbf{N}}\mathbf{v}^T\right) \right] + \tilde{\mathbf{N}}P + r\,\mathbf{g} = \mathbf{0} \tag{2}$$

where $\mathbf{v}$ and P are the mean values of the velocity and pressure fields; μ and ρ are liquid steel viscosity and density and $\mathbf{g}$ is gravity acceleration. μ^t is the turbulent or eddy viscosity, whose expression in terms of the mean velocity is given by the turbulence model.

Two different ways of estimating the turbulent viscosity are used: the (k-L)-predictor /(e)-corrector turbulence model and the mixing length model. The code FANTOM [22] is applied to integrate the non-linear system of equations by the finite element method [23]. Isoparametric standard finite elements, penalisation of the pressure and the Streamline Upwind Petrov Galerkin technique are applied [23-24].

2.1. Mixing length turbulence model

In the mixing length turbulence model [19], the turbulent viscosity is obtained from the velocity gradient through the following expression:

$$m^t = \rho l^2 (\nabla \mathbf{v} : \nabla \mathbf{v} + \nabla \mathbf{v} : \nabla \mathbf{v}^T)^{1/2} \tag{3}$$

where l is the mixing length which must be set a priori. The mixing length model is called a "zero equation" model because no differential equation is necessary to calculate the turbulent viscosity.

2.2. (k-L)-predictor /(ε)-corrector turbulence model

The k-ε model was developed by Launder and Spalding [16] and two new unknown variables are introduced: k and ε. A transport differential equation must be applied to calculate each variable, as follows:

$$\rho \frac{\partial k}{\partial t} + \rho \mathbf{v} \cdot \tilde{\nabla} k - \tilde{\nabla} \cdot \left[\left(\mu + \frac{\mu^t}{\sigma_k} \right) \tilde{\nabla} k \right] - \mu^t \left(\tilde{\nabla} \mathbf{v} + \tilde{\nabla} \mathbf{v}^T \right) : \tilde{\nabla} \mathbf{v} + \rho \frac{C_\mu k^2}{\mu^t / \rho} = 0 \tag{4}$$

$$\rho \frac{\partial \varepsilon}{\partial t} + \rho \mathbf{v} \cdot \tilde{\nabla} \varepsilon - \tilde{\nabla} \cdot \left[\left(\mu + \frac{\mu^t}{\sigma_\varepsilon} \right) \tilde{\nabla} \varepsilon \right] - \rho C_\mu C_1 k \left(\tilde{\nabla} \mathbf{v} + \tilde{\nabla} \mathbf{v}^T \right) : \tilde{\nabla} \mathbf{v} + \rho \frac{C_2 \varepsilon^2}{k} = 0 \tag{5}$$

The k-ε model is based on a series of constants, which were determined by calibration with experimental results [16]. The values of these constants are $C_m = 0.09$, $C_1 = 1.44$, $C_2 = 1.92$, $\sigma_k = 1.0$ and $\sigma_\varepsilon = 1.0$.

In the present work, the (k-L)-predictor /(ε)-corrector algorithm developed in previous publications [17-18] is used for the implementation of the k-ε model. This algorithm calculates the turbulent viscosity through the following expression:

$$\mu_t = C_\mu \rho \sqrt{k}\, L \tag{6}$$

where $L = \frac{k^{3/2}}{\varepsilon}$ is the length scale.

Our iterative scheme loops between a predictor phase (k-L model, Eqs. (1,2,4)) and a corrector phase (ε transport equation, Eq. (5)) and updates the value of L using an under relaxation technique. A complete description of (k-L)-predictor / (ε)-corrector algorithm is found in our publications [17-18].

2.3. Interface model

In flows with free surface or with two different fluids, there is an interface which is unknown and must be found as part of the solution. In order to track the position of the interface, the pseudoconcentration method [10] is adopted in this paper.

In this method the Eqs.(1-6) are solved in the domain of interest together with an equation for an additional unknown, the pseudoconcentration C, that satisfies the following advection equation:

$$\frac{\partial C}{\partial t} + \mathbf{v} \cdot \tilde{\mathbf{N}} C = 0 \tag{7}$$

$C(\mathbf{x},t) = C_c$ Corresponds to the interface between fluid 1 and fluid 2

$C(\mathbf{x},t) > C_c$ Corresponds to the region occupied by the fluid 1

$C(\mathbf{x},t) < C_c$ Corresponds to the region occupied by the fluid 2

where C_c is an arbitrary critical value.

Eq. (7) is solved using isoparametric finite elements, a Streamline Upwind Petrov Galerkin technique and an implicit method to iterate in time [24-25]. The initial position of the interface determines the initial choice of the value of C. Appropriate boundary conditions are used at the inlet and outlet.

It is evident that infinite possible pseudoconcentration functions may correspond to each position of the interface. However, the pseudoconcentration must be a smooth function of position in order to avoid numerical problems. Therefore, after updating the position of the interface, the pseudoconcentration is smoothed keeping the position of the interface with the following expression:

$$C(\mathbf{x},t) = C_c + d \; \boldsymbol{s} \; \mathrm{sgn}\left(C(\mathbf{x},t) - C_c\right) \tag{8}$$

In Eq. (8), d represents the distance to the interface and $\boldsymbol{s}$ is an arbitrary constant. The algorithm that calculates d behaves in the following way:

- Within each element intersected by the interface, the interface is approximated by a plane.
- The distance from any given node in the mesh to each interface plane is calculated.

- The minimum of these distances is taken as d for the given node.

The same procedure is applied to free surface problems, where the density and viscosity are chosen so that the air (pseudofluid) effects on the fluid are negligible.

2.4. Wall boundary conditions

Turbulence models do not represent properly the flow near solid walls where viscous effects are dominant. To prevent numerical problems in the neighbourhood of rigid walls, the wall functions method is used [16]. The basic idea of the method is not to solve the turbulence model equations in the boundary layer but to use general empirical laws instead. The domain where the equations are solved is moved away from the walls a short distance (D).

A complete description of the algorithm we used to impose wall functions as boundary conditions may be found in [17]. Boundary conditions for the stress and turbulent variables on a point "P" of the computational domain near the wall are imposed by the relations:

$$\tau_w = U_*^2 \rho \quad ; \quad k_P = \frac{U_*^2}{\sqrt{C_m}} \quad ; \quad \varepsilon_P = \frac{U_*^3}{\kappa \Delta} \tag{9}$$

where $\kappa = 0.4$ is the Von Karman constant. U_* is the friction velocity which is related to the tangential velocity at "P" by the equation:

$$U_P = \frac{U_*}{\kappa} \ln \frac{\rho E U_* \Delta}{\mu} \tag{10}$$

where E is a function of the wall rugosity (typically $E = 9$).

3. WATER MODEL SIMULATION

In order to verify our numerical turbulence model for flows with an interface, a scaled down water model of a slab mold developed by Keicher and Taylor [20-21] and found in the literature [25-26] is simulated. The surface of water in the mold is covered with a layer of oil to represent the molten flux powder on the liquid steel in the continuous casting process.

The shape of the final casting product is determined by the mold geometry, which in this case is a rectangular section of different thicknesses and widths. It is important to know how the surface of steel in the mold is affected by the flow entering the mold, for different geometrical configurations. The mold is filled with steel through the submerged entry nozzle (SEN). In order to maintain the liquid steel level in the mold, the velocity of the steel at the SEN entrance must be proportional to the "casting speed" (the speed at which the slab is removed from the caster by the rolls).

In Table 1 geometrical data of the experiments are presented.

Table 1. Water model experiment [20-21]

Mold width	*0.457 m*
Mold thickness	*0.059 m*
Nozzle immersion depth	*0.150 m*
Nozzle internal diameter *(d_{SEN})*	*0.0195 m*
Nozzle external diameter	*0.0295 m*
Nozzle port angle	*20°*
Vertical modelled length	*0.686*
Oil layer thickness	*0.065*

In Fig. 2, a scheme of the central section of the mold is presented. Only one fourth of the mold-SEN is modelled, since the problem is symmetric. Turbulence is taken into account using the *k-ε* model. The parameters of Eq. (8) are chosen as $C_c = 0.5$; $\sigma = 0.015$ and *C* ranges from *0* to *1*.

The boundary conditions in the model are:

- ✓ Dirichlet boundary conditions at the SEN entrance: $V_{in} = 1.560$ or 0.890 *m/s* ; $C_{in} = 1.0$, $k_{in} = 0.00425\, V_{in}^2$; $\varepsilon_{in} = k_{in}^{3/2}/d_{SEN}$.
- ✓ Wall functions at the rigid walls.
- ✓ Symmetry boundary conditions on symmetry planes.

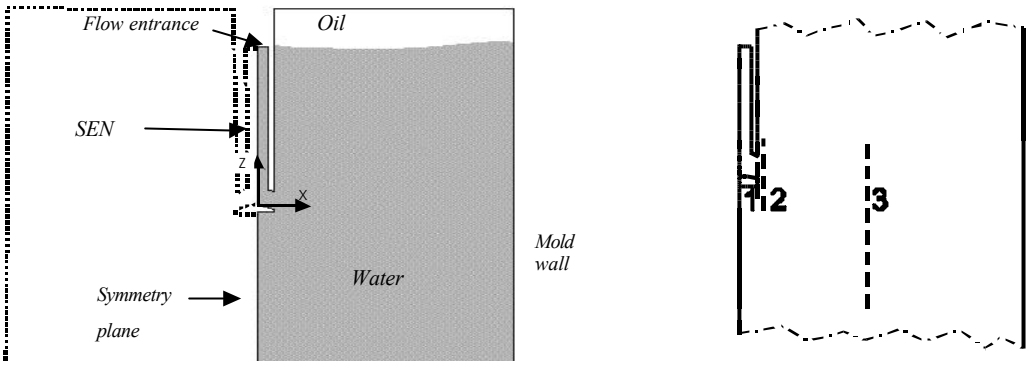

Figure 2. Modelled domain. Position of the lines 1, 2 and 3 where the comparison between the experimental water model and the numerical method is presented

A modified pressure is introduced by $P'(x,y,z)=P(x,y,z)-P_0(z)$, where $P(x,y,z)$ is the actual pressure and $P_0(z)$ is the hydrostatic pressure which only depends on the vertical coordinate. Homogenous modified pressure boundary conditions are applied on both the upper and lower limits of the mold domain. A force term $\nabla p_0 = -\boldsymbol{g}\, \boldsymbol{r}_0(z)$ is included in the Navier-Stokes equation to compensate the use of the modified pressure ($\boldsymbol{r}_0$ is the initial hydrostatic distribution of densities).

Following the experimental results, two simulations are carried out. First, the water flow with a fixed surface is modelled to compare the velocity field. Then, the flow with water and oil is simulated to analyse the behaviour of the free interface.

A 3-D mesh with 23379 nodes and 19100 isoparametric hexahedral linear elements and the properties showed in the Table 2 are used in the numerical simulation.

Table 2. Properties of the fluids used in the experimental simulation

	Water	*Olive oil*
Density [Kg/m^3]	1000.0	918.0
Viscosity [N s/ m^2]	0.001	0.0991

3.1. Fixed surface simulation

This case is simulated to investigate the velocity field and compare results with experimental measurements taken from the literature [26].

The three vertical lines placed at different distances from the nozzle on the symmetry plane (see Figure 2) are used to compare the experimental water model results [26] (points) and the numerical results (full lines) as shown in Figure 3. Non-dimensional values are defined by

$$v_x^* = \frac{v_x}{v_{in}} \quad ; \quad v_z^* = \frac{v_z}{v_{in}} \quad ; \quad z^* = \frac{z}{d_{SEN}} \tag{11}$$

where v_x is the horizontal velocity; v_z is the vertical velocity; z is the vertical coordinate; $z = 0$ is the floor of the SEN; and d_{SEN} is the internal diameter of the SEN.

The numerical results match the experimental ones satisfactorily showing that the k-ε turbulence model can be successfully applied to describe the flow inside the mold.

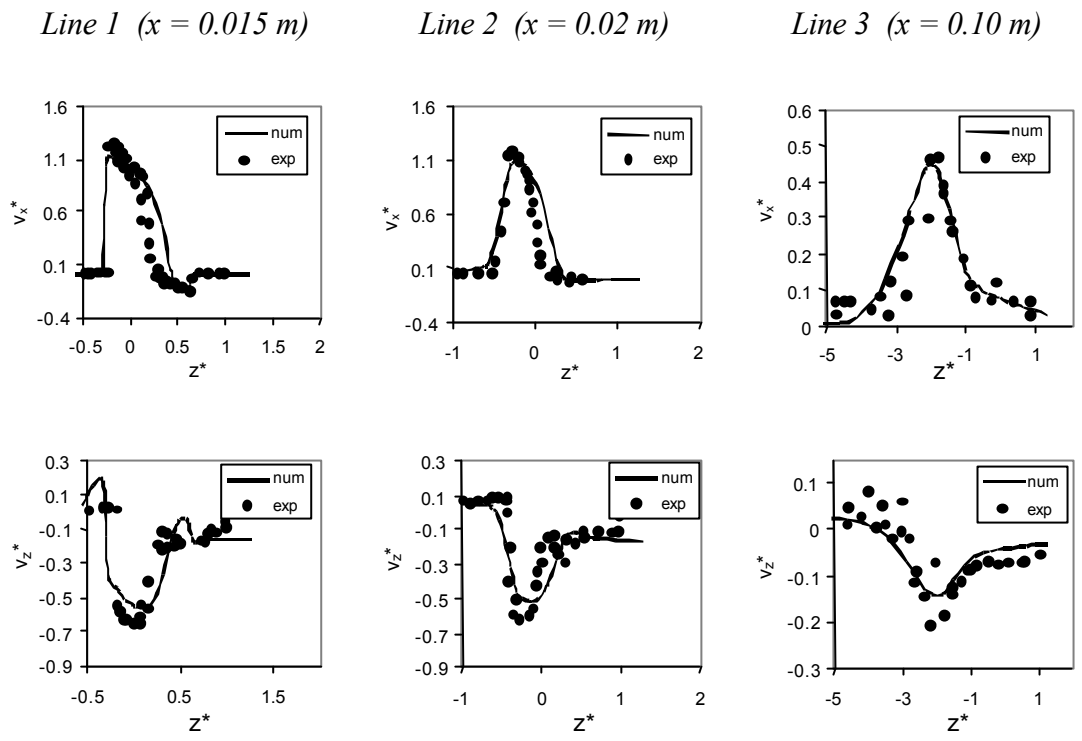

Figure 3 – Comparison between the measured [26] and calculated horizontal (v_x^*) and vertical (v_z^*) components of velocity. The abscissas axis z^* corresponds to vertical lines placed inside the mold at different distances from the nozzle (see Figure 2).

3.2. Water – oil interface

Validation of the numerical interface profile between water and oil is also carried out by comparison with experimental results presented in reference [26].

Figure 4 shows numerical interface profile results. The interface has the form of a standing wave with its maximum at the narrow mold wall. No differences of interface height can be appreciated across the thickness of the mold. In Fig. 5 the interface profile at the symmetry plane is compared to experimental results.

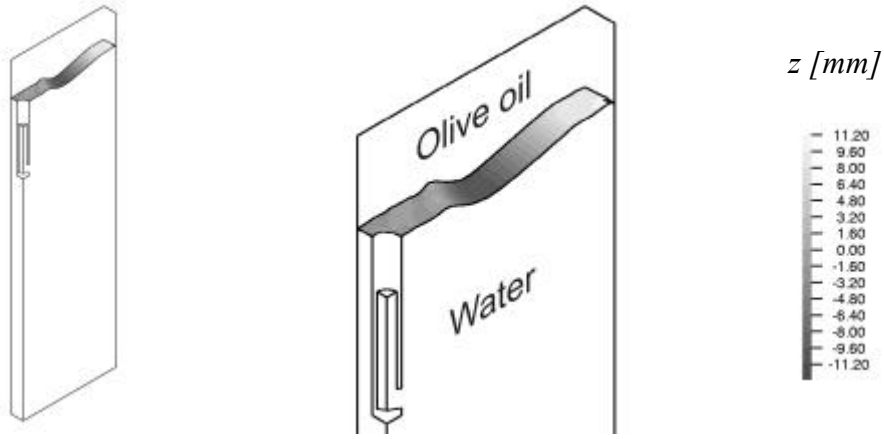

Figure 4. Results of the numerical simulation for the water model with an oil layer. The grey scale represent the height of the interface with respect to the unperturbed position

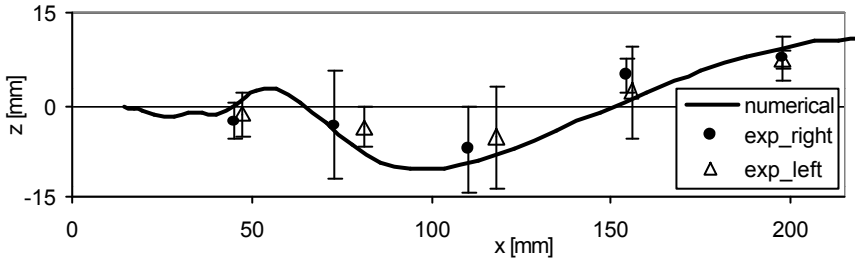

Figure 5 – Comparison between numerical and experimental [26] interface profile results

4. INDUSTRIAL SIMULATIONS

Two steps during the continuous casting process are simulated: the liquid steel flow inside a slab mold and the liquid steel drainage of the ladle.

4.1. Design of a submerged entry nozzle for a slab mold

The first industrial example to be analysed is the flow of steel inside a slab mold used at SIDERAR, San Nicolas, Argentina. The interface steel-molten flux powder can become unstable for high values of the casting speed, depending on nozzle and mold design. We are interested in the steady state profile of the interface.

The continuous caster used at SIDERAR is shortly going to increase its casting speed. Therefore, it is necessary to understand the consequences that this increase may have on the fluid dynamics in the upper part of the mold. It is also relevant to analyse alternative SEN designs that can help to prevent the difficulties that may arise.

Table 3. Mold and SEN data

Mold height	*0.8 m*
Mold width	*1.0 m*
Mold thickness	*0.2 m*
Nozzle immersion depth	*0.157 m*
Nozzle internal diameter	*0.063 m*
Nozzle external diameter	*0.1 m*
Nozzle port angle	*15°*
Vertical modelled length	*2.8 m*
Molten flux powder layer thickness	*0.035 m*

Four different SEN designs are modelled for a high casting speed of *2 m/min*. The first one corresponds to the SEN presently used at SIDERAR, which only discharges the liquid steel into the mold through two lateral ports. The other three alternative designs are essentially equal to the previous one but they also have a hole in the bottom that allows part of the liquid steel to flow vertically into the mold. The sizes of the holes are *15*, *25* and *35 mm* respectively. The main characteristics of the modelled SEN and the mold are given in Table 3.

A 2-D mesh with 10919 nodes and 10628 isoparametric quadrilateral linear elements is used for the numerical simulation. Taking into account symmetry conditions only half of the mold is modelled. The density and viscosity of both fluids are given in Table 4.

Table 4. Properties of the fluids used in the industrial simulation

	Liquid steel	*Molten flux powder*
Density [Kg/m^3]	7000.0	2500.0
Viscosity [N s /m^2]	0.0067	0.1

In Figure 6 the velocity modulus is shown together with a schematic representation of the flow pattern. It can be seen that for SEN without a vertical discharge port the flow forms two large recirculation zones. In the bottom one the liquid steel first flows downwards close to the narrow wall of the mold and then part of the flow moves upwards at the centre of the mold. The top recirculation loop is formed by the liquid steel that reaches the narrow wall of the mold and then flows towards the liquid steel–molten flux powder interface. The intensity of this recirculation is a key factor in order to avoid instabilities at the interface that can lead to defects.

With a *15 mm* diameter vertical discharge port, a third recirculation is formed. Nevertheless, this recirculation is quite weak and the flow inside the mold is relatively similar to the one described for the previous case. The recirculation formed in the upper part of the mold is weaker than the one obtained without a vertical discharge port.

When the diameter of the vertical port increases to *25 mm,* the flow in the upper part of the mold is not affected significantly. The flow through the vertical port increases and the two lower recirculations have approximately the same intensity and extent.

Finally, with a *35 mm* discharge port, the most significant change takes place. The recirculation in the upper part of the mold disappears, and the flow that comes out of the lateral port is dragged by the flow that comes out of the vertical port. The liquid steel flows downwards at the centre of the mold and raises close to the narrow wall.

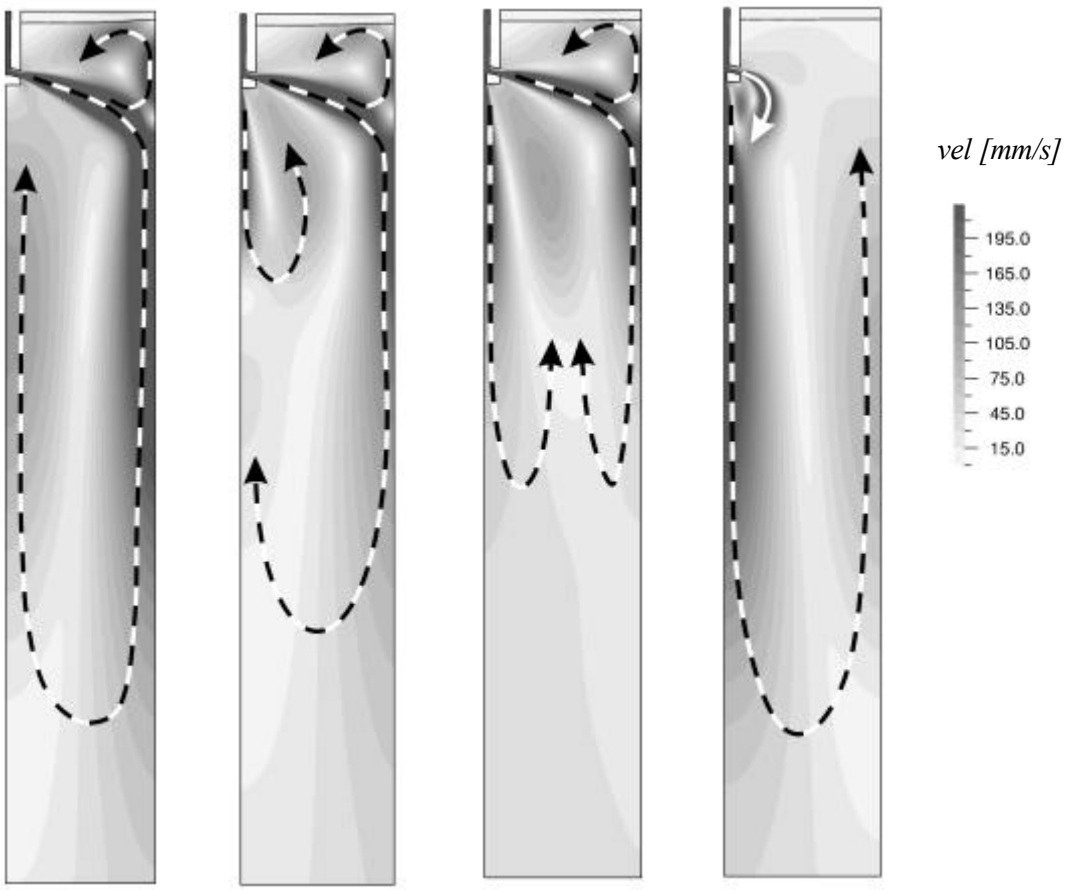

Figure 6 - Velocity distribution for different SEN with lateral port (48 x 64 mm) and different vertical hole.

In Figure 7 the shape of the interface between liquid steel and molten mold powder is shown. The SEN without a vertical port produces the highest wave; this is obviously related to the high intensity of the upper recirculation. The height of the wave obtained with a *15 mm* port is very similar to the one obtained with a *25 mm* port and approximately half of the one obtained without a vertical port. With a *35 mm* vertical port the interface remains nearly unaltered, since there is no upper recirculation.

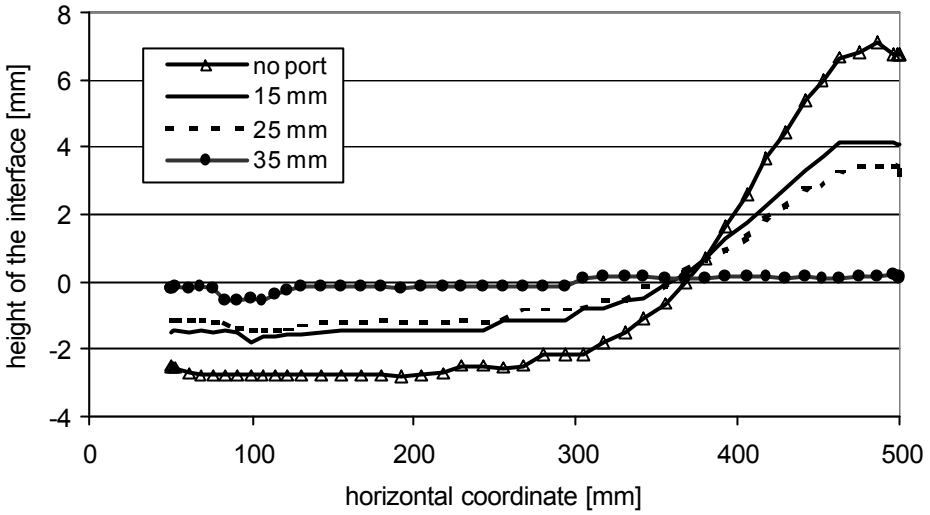

Figure 7 - Shape of the liquid steel-molten flux powder interface

These preliminary results indicate that the flow in the mold depends strongly on the shape of the SEN. The cases with vertical discharge ports of either *15* or *25 mm* help to reduce the intensity of the upper recirculation without altering the flow pattern significantly. Therefore they seem to be valid alternatives for a SEN with high continuous casting velocity. The SEN with a *35 mm* vertical port eliminates the upper recirculation, giving place to the formation of a dead zone that will surely lead to the cooling of the liquid steel and thus making it a not valid choice.

4.2. Liquid steel drainage of a ladle

The second industrial problem to be analysed is the drainage of a ladle. The industrial ladle to be considered belongs to SIDERAR steelmaking plant at San Nicolás, Argentina. It has an oblong section instead of the usual circular section, its discharge is close to the wall and its floor is inclined towards the discharge. The latter characteristic reduces the amount of

steel left over in the ladle when the critical height is reached (the critical height is the height of the unperturbed interface when the free surface irruption in the nozzle takes place).

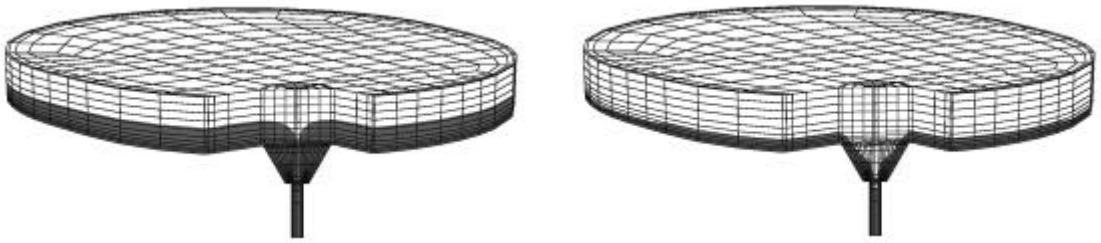

Figure 8 - Teeming of an industrial ladle.

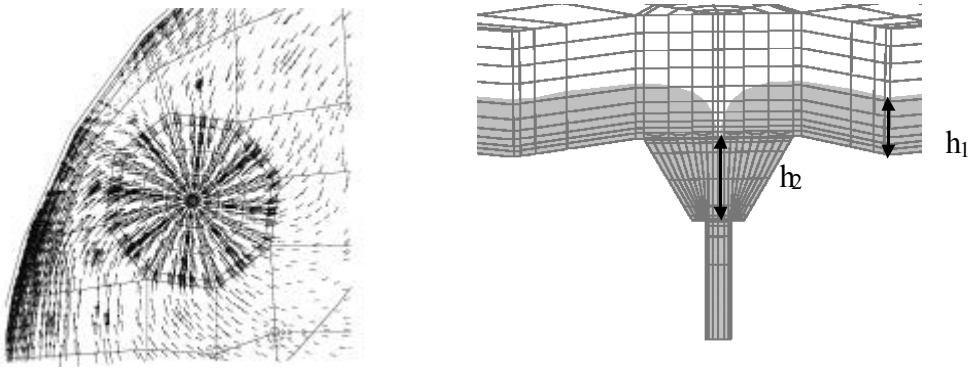

Figure 9 – Velocity profile and surface deformation near the ladle's nozzle.

The mesh is composed by 4260 isoparametric hexahedral elements and 4957 nodes. It is coarse throughout most of the ladle and fine in the neighbourhood of the discharge. Liquid steel properties ($\mu = 0.0053 N\ s/\ m^2$, $\rho = 7500\ Kg/m^3$) are used to carry out the calculations. Since in this case we are dealing with a free surface problem, the properties of the pseudofluid were chosen 1000 times smaller than those of liquid steel so that the effects

on the flow are negligible. The mixing length model is used to represent turbulent effects. The main characteristics of the modelled ladle are given in Table 5.

Table 5. Ladle data

Ladle height	*4.0 m*
Modeled ladle height	*0.3 m*
Minimum bottom diameter	*2.9 m*
Maximum bottom diameter	*3.3 m*
Minimum top diameter	*3.2 m*
Maximum top diameter	*3.6 m*
Nozzle diameter	*0.07 m*

Figures 8 and 9 show the numerical results. No vortex is formed and the irruption of the air at the outlet occurs when the height of the steel column is comparable to the diameter of the nozzle. The amount of steel left in the ladle according to the model is in agreement with the usual values of wasted tons of steel in the industrial ladle.

In Fig. 10 the time evolution of the height of the free surface in two different points is plotted. The height of the column of steel away from the region affected by the surface deformation is h_1 (see Figure 9). The "funnel height", defined as the distance from the lower point of the deformed free surface to the ladle's nozzle, is h_2 (see Figure 9). The irruption of the free surface in the nozzle takes place when h_2 becomes negative. Time

$t = 0$ corresponds to the beginning of the simulation with a $0.2\ m$ height column of steel and unperturbed free surface.

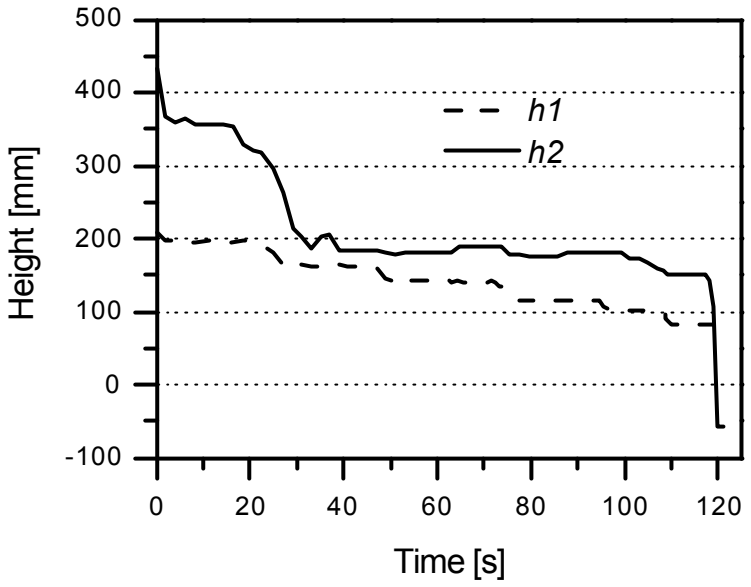

Figure 10 – Time evolution of the steel column height h_1 and funnel height h_2 (see Figure 9)

Though the results have not yet been validated with experiments, the model can simulate the draining process in agreement with observation [27-28]. Our current numerical simulations on ladles with centred discharge and initial rotation show vortex formation even when a high column of liquid still remains in the ladle. Both phenomena, funnel formation without vortex in ladles with eccentric discharge and vortex formation in ladles with central discharge and initial rotation, are consistent with available observations [27-28]. Final validation of the numerical model –in the context of ladle teeming- is being carried out with experiences developed at Buenos Aires University.

5. CONCLUSIONS

A numerical model for turbulent flows with an interface between two fluids has been developed. The model uses the finite element method on a fixed grid together with the pseudoconcentration technique to capture the position of the interface. Two turbulence models are used: the k-ε turbulence model and the mixing length model.

Since measurements of the fluid dynamics during the steelmaking process are difficult and expensive (high temperatures and visual opacity of liquid steel), the validation has been done with experimental data from a water model.

The numerically calculated shape of the oil-water interface in the mold agrees satisfactorily with the experimental values showing that the model can provide quantitatively valid predictions for the steady state behaviour of the interface.

Even though there are still no quantitative comparisons for the shape of the interface during the drainage of the ladle, visual observations and predictions for the amount of steel left over in the ladle during the industrial process indicate that the model can also be applied to this operation. The final validation of the model in the context of ladle teeming, that is being carried out with a water model, will provide higher confidence on the numerical results for this transient case.

The industrial simulation of the flow in a slab mold is an example of how the model can be used to obtain a better understanding of the complex processes that take place inside the continuous caster. The numerical tools can help to reduce trial and error during the design of a new component or process; in this case the SEN.

Acknowledgements

The authors gratefully acknowledge the financial support of SIDERAR (San Nicolas, Argentina), SIDOR (Puerto Ordaz, Venezuela) and the companies of the TENARIS group: SIDERCA (Campana, Argentina), TAMSA (Veracruz, Mexico) and DALMINE (Dalmine, Italy).

REFERENCES

1 Goldschmit, M.B., Príncipe, R.J. and Koslowski, M. (1999) 'Applications of a (k-ε) model for the analysis of continuous casting processes', *International Journal for Numerical Methods in Engineering*, Vol. 46, pp. 1505-1519.

2 Goldschmit, M.B. and Coppola Owen, A.H. (2001) 'Numerical modeling of gas stirred ladles', *Ironmaking and Steelmaking*, Vol. 28, pp. 337-341.

3 Goldschmit, M.B., Ferro, S.P. and Mazzaferro, G. (2002) 'Numerical modeling of liquid steel flow with free surface', *4th. European continuous Casting Conference*, Birmingham, UK, (in Press).

4 Gonzalez, M., Fernández Berdaguer, E, Goldschmit, M.B. and Dvorkin, E.N. (2001) 'Evaluation of the heat transfer coefficients in the mold of a steel slabs continuous casting installation', *IX Reunión de Trabajo en Procesamiento de la Información y Control*, Santa Fe, Argentina.

5 Reza Aboutalebi, M., Hasan, M. and Guthrie, R.I.L. (1995) 'Coupled turbulent flow, heat, solute transport in continuos casting processes', *Metallurgical and Material*

Transactions B, Vol. 26B**,** pp. 731-744.

6 Maldovan, M., Príncipe, J., Sánchez, G., Pignotti, A. and Goldschmit, M.B. (2000) 'Numerical modeling of continuous casting of rounds with electromagnetic stirring', *European Congress on Computational Methods in Applied Sciences and Engineering*, ECCOMAS 2000, Barcelona, Spain.

7 Mazumdar, D. and Guthrie, R.I.L. (1999) 'The physical and mathematical model of continuous casting tundish systems', *ISIJ International* , Vol. 39, pp. 524-547.

8 Hughes, T., Liu, W. and Zimmerman T. (1981) 'Lagrangian-Eulerian finite element formulation for viscous flows', *Comput. Methods Appl. Mech. Engrg.*, Vol. 29, pp. 329-349.

9 Radovitzky, R. and Ortiz, M. (1998) 'Lagrangian finite element analysis of newtonian fluid flows', *Int. J. Numer. Meth. Engng.*, Vol. 43, pp. 607-619.

10 Thompson, E. (1986) 'Use of the pseudo-concentrations to follow creeping viscous flows during transient analysis', *Int. J. Num. Meth. Fluids*, Vol. 6, pp. 749-761.

11 Cavaliere, M.A., Goldschmit, M.B. and Dvorkin, E.N. (2000) 'On the solution of coupled thermo-mechanical problems via the pseudoconcentration technique', *European Congress on Computational Methods in Applied Sciences and Engineering*, ECCOMAS 2000, Barcelona, Spain.

12 Tezduyar, T. (2001) 'Finite element methods for flow problems with moving boundaries and interfaces', *Archives of computational methods in engineering*, Vol. 8, No. 2, pp. 83-130,

13 Mohapatra, P., Murty Bhallamudi, S. and Eswaran, V. (2001) 'Numerical study of flows with multiple free surfaces', *Int. J. Numer. Meth. Fluids*, Vol. 36**,** pp. 165-184.

14 Iafrati, A., Di Mascio, A. and Campana, E. (2001) 'A level set technique applied to

unsteady free surface flows', *Int. J. Numer. Meth. Fluids*, Vol. 35, pp. 281-297.

15 Vincent, S. and Caltagirone, J. (1999) 'Efficient solving method for unsteady incompressible interacial flow problems', *Int. J. Numer. Meth. Fluids*, Vol. 30, pp. 795-811.

16 Launder, B.E. and Spalding, D.B. (1974) 'The numerical computation of turbulent flows', *Comp. Meth. in Appl. Mech. and Engrg*., Vol. 3, pp. 269-289.

17 Goldschmit, M.B. and Cavaliere, M.A. (1995) 'Modelling of turbulent recirculating flows via an iterative (k-L)-predictor /(ε)-corrector scheme', *Applied Mechanics Review*, Vol. 48, pp. 11.

18 Goldschmit, M.B. and Cavaliere, M.A. (1997) 'An iterative (k-L)-predictor / (ε)-corrector algorithm for solving (k-ε) turbulent model', *Engineering Computations*, Vol. 14, No. 4, pp. 441-455.

19 Speziale, C. G. (1991) 'Analytical methods for the development of Reynolds-stress closures in turbulence', *Annu. Rev. Fluid Mech*., Vol. 23, pp. 107-157.

20 Keicher, M. and Taylor, A. (1997) unpublished research, Imperial College, London.

21 Keicher, M. (1997) 'Physical modelling of the Continuous Casting Process', Technical Report TF 97/06, MED, Imperial College, London.

22 FANTOM (1994) *User manual*, International Center for Numerical Methods in Engineering, Barcelona, Spain.

23 Zienkiewicz, O.C. and Taylor, R.L. (2000) *The Finite Element Method*, Butterworth-Heinemann, London.

24 Brooks, A.N. and Hughes, J.R. (1982) 'Streamline upwind Petrov-Galerkin formulations for convection dominated flows with particular emphasis on the

incompressible Navier-Stokes equations', *Comp. Meth. in Appl. Mech. and Engrg*., Vol. 32, pp. 199-259.

25 Panaras, G.A., Theodorakakos, A. and Bergeles, G. (1998) 'Numerical investigation of the Free Surface in a Continuous Steel Casting Mold Model', *Metallurgical and Material Transactions B*, Vol. 30B**,** pp. 1117-1126.

26 Anagstopoulos, J. and Bergeles, G. (1999) 'Three-Dimensional Modelling of the Flow and the interface Surface in a Continuous Casting Mould Model', *Metallurgical and Material Transactions B*, Vol. 30B, pp. 1095-1105.

27 Koria, S.C. and UmaKanth, (1994) 'Model studies of slag carry-over during drainage of metallurgical vessels', *Steel Research*, Vol. 65, pp. 8-14.

28 Sankaranarayanan, R. and Guthrie, R.I.L. (1992) 'A laboratory study of slag entrainment during the emptying of metallurgical vessels', *Steelmaking Conf. Proc*., *ISS-AIME*, Vol. 75, pp. 655-664.